ISSN 2176-5480

22nd International Congress of Mechanical Engineering (COBEM 2013)
November 3-7, 2013, Ribeirão Preto, SP, Brazil

APPLICATION OF STRUCTURAL RELIABILITY METHODS TO STOCHASTIC FATIGUE PROBLEMS - A STUDY FOR STEEL ASTM A743 CA6NM

Erich Douglas de Souza
erich.d.souza@gmail.com
Departamento de Engenharia Mecânica, Universidade de Brasília – Campus Universitário Darcy Ribeiro, Asa Norte, Brasília, DF, Cep.: 70910-910, Brasil.

Jorge Luiz de Almeida Ferreira
jorge@unb.br
Departamento de Engenharia Mecânica, Universidade de Brasília – Campus Universitário Darcy Ribeiro, Asa Norte, Brasília, DF, Cep.: 70910-910, Brasil.

José Alexander Araújo
alex07@unb.br
Departamento de Engenharia Mecânica, Universidade de Brasília – Campus Universitário Darcy Ribeiro, Asa Norte, Brasília, DF, Cep.: 70910-910, Brasil.

Abstract. *This paper presents a study about the structural integrity of ASTM a743 CA6NM. This component is essential in the structural integrity of the hydro generator and was chosen for being susceptible to cracks initiation. In this sense, the main failure mode is fatigue and the functions which characterize the material strength, capacity, and the load history applied to the blade, demand, were determined. Three demand functions were built, one based on Goodman's diagram, one based on Gerber's diagram, and another based on the Walker's equation. The parameters that characterize capacity function were obtained by means of tensile and fatigue tests. For the characterization of the stress loading history applied on the blade, a finite element analysis was used. Based on those results, safety factor, reliability index and reliability of the blade were considered. The reliability index and the reliability were estimated according to FORM, SORM and Monte Carlo techniques. The results reveal that the blade is not likely to fail under the conditions simulated.*

Keywords: *fatigue failure, FORM, SORM, Monte Carlo simulation.*

1. INTRODUCTION

In Kaplan hydro turbines the water flow is regulated by the distributor blades and by the turbine blades inclination. This makes difficult to build a proper model for large perturbations regarding the problem's characteristic variables. The complex geometry and the transient characteristics of the flow also make more difficult to realize a simulation to capture all these singularities. These effects are extremely complex to be numerically simulated and with no analytical solution. These components working under cyclic loads need an evaluation of the structural integrity reliability, which is the capacity of certain structural element to support cycles of loads in a determined period of time they were designed for.

The fatigue damage is a continuous and cumulative process that can be defined as the loss of functionality of a structural component working under cyclic loads. The fatigue damage is considered null in virgin materials and evolutes to a critic value, Dc, which characterizes the growth of microscopic cracks in the material, and can be measured by the load history and the utilization of constitutive equations which predict the necessary number of load cycles to the initiation of the cracks. The effect of stress concentration may causes a fast propagation of the crack, causing an increase of the local stress until failure occurs. Therefore the fatigue failure is sudden and total, and its prediction of great importance when designing machines and components which work under cyclic loads, and even more when there are combined loads, flexion and torsion, applied alternatively and repetitively.

The analysis of structural reliability of the turbine blade was based in a fatigue failure trough the Goodman, Gerber and Walker uniaxial criteria. The capacity parameters were the properties of the material of the blade. The demand parameters were the results of the static pressure distribution over the blade obtained by a CFD simulation, using the CFX software. For the fatigue failure criteria, a transient analysis was performed using the ANSYS software. The static pressure distributions over the blade were applied like a unit step function. The stress history on the blade was used to identify the critic regions and use the stress amplitudes as demand parameter to the reliability analysis based on fatigue failure criteria.

ISSN 2176-5480

2. UNIAXIAL FATIGUE MODELS

A common approach to evaluate the mean stress effect on fatigue life is by analyzing diagrams of mean stress, S_m, versus alternating stress, S_a. In that sense, several combinations of mean and alternating stress, that cause fatigue failure of the specimen when subjected to N cycles of constant amplitude load, are plotted for a specific fatigue life. The most used models to represent this mean stress effect are the ones proposed by Goodman and Gerber. Using these models, it is possible to determine the fatigue strength limit of the material when subjected to loads described by an alternating stress S_a and mean stress S_m, as presented in Eq. (1).

$$S_{ar} = \frac{S_a}{1 - \left(\frac{S_m}{S_{ut}}\right)^{\alpha}} \tag{1}$$

where S_{ar} is the fatigue strength limit, S_{ut} is the ultimate strength for the material and α is equal to one for the linear relation of Goodman (1899), and two for the parabolic expression of Gerber (1874).

At the end of the sixties, Smith-Watson-Topper (Smith, 1970) proposed the empirical relation presented in Eq. (2) as an attempt to quantify the mean stress effect on fatigue life, where Δε/2 represents the alternating strain and E the Young modulus of the material, σ'_f is the fatigue strength and N is the number of cycles.

$$S_{max} \cdot \frac{\Delta\varepsilon}{2} = \frac{(\sigma'_f)^2}{E} \cdot (N)^{2b} \tag{2}$$

Rearranging this last relation, and correlating the fatigue strength limit, S_{ar}, to the parameters that describe the load, the Eq. (2) can be expressed as Eq. (3):

$$S_{ar} = S_a \cdot \sqrt{\frac{2}{1-R}} \tag{3}$$

were R is defined as the quotient of the maximum and minimum stresses in a load cycle.

Using the same philosophy adopted by Smith-Watson-Topper, Walker (Walker, 1970) proposed the relation presented in Eq. (4) to quantify the fatigue strength limit, S_{ar}, where the parameter γ is a constant characteristic of the material.

$$S_{ar} = S_a \cdot \left(\frac{2}{1-R}\right)^{1-\gamma} \tag{4}$$

In these models the Eq. (1), (3) and (4) define the limits of the fatigue failure region for a specific life, N. If the point representative of the stress cycle, (S_m, S_a), or (R, S_a), is located in the region between the Cartesian axes and the representative curves, there should not be failure based on such criterions. The graph shown on Fig. 1 exemplifies the behavior of the discussed models, the lines indicating hypothetical tests assuming load ratios of magnitude R and, as well as the geometrical places of the pair (S_m ,S_a) that represents the limits of failure.

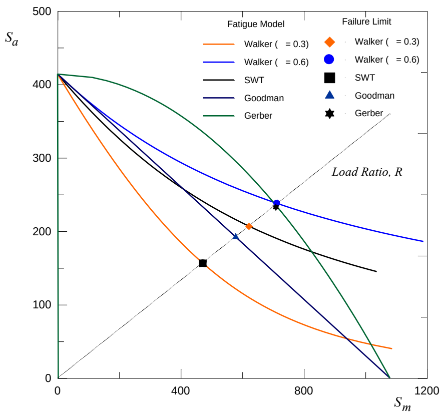

Figure 1 - Fatigue Models Representative Curves

ISSN 2176-5480

3. RELIABILITY MODELS IN THE UNIAXIAL CONTEXT

Reliability is the capacity of a certain machine or component to resist to the conditions and time they were designed and build, under maximum test and work loads during its life. According to Harr (1987), reliability or safety can be defined as the probability of success of a system in working under operation conditions in a specific period of time. The operations conditions or system's capacity are commonly called demands. To define an acceptable level of reliability a structure must have, the cost-benefits and risks associated to it are taken in consideration. Traditionally in engineering the safety factor is used to evaluate the risks of failure, which estimative is done considering Eq. (5):

$$FS = \frac{\bar{C}}{\bar{D}} \tag{5}$$

where $\bar{C}$ is the mean capacity and $\bar{D}$ is the mean demand (Shen and Soboyejo, 2001). To conclude weather the safety factor is high enough for the structure to bear the demands, it must be compared to experimental values of the factor obtained for the same model. Assuming that C and D have normal distributions, the limit state function (LSF) Z will also have normal distribution, and can be defined as Eq. (6). Defining the X_i´s variables associated to the capacity and demand functions, the failure probability estimative is built in base on a limit state equation, g (X).

$$Z = g(X) = g(X_1, X_2, X_3, \ldots, X_n) \tag{6}$$

Z is called safety margin function and defined as:

$$Z = C - D \tag{7}$$

Varying the values of X_i, the function of limit state g (X) can assume the following conditions: g(X) > 0, no failure will occur; g (X) = 0, limit state, eminence of failure; g (X) < 0; failure will occur. Usually, the limit state can be a function with capacity and demand variables. The following integration defines the probability of failure:

$$P_f = Prob[g(\boldsymbol{X}) \le 0] = \int_{g(\boldsymbol{X}) \le 0} f(\boldsymbol{X}) d\boldsymbol{X} \tag{8}$$

The function f (X) is the probability density function of the variables X_i´s. Another measure of adequacy of a design is the reliability index:

$$\beta = \frac{\bar{Z}}{\sigma_Z} = \frac{\bar{C} - \bar{D}}{\sqrt{\sigma_C^2 + \sigma_D^2}} \tag{9}$$

The reliability evaluate can be done entirely by the comparison of the reliability index β, to those considered adequate, based in previously experiments with the structure studied. If Z can be assumed as a normal random variable, the failure probability is:

$$P_f = \Phi(\beta) \tag{10}$$

where Φ is the cumulative distribution function for a standard normal variable:

$$\Phi(\beta) = \int_{-\beta}^{+\infty} f(X)\, dX \tag{11}$$

It will be used an approximate probabilistic methodology to solve this integral. The approximate methods simplify the functional relations among the state variables and the problem. In this way, the failure probability is only an approximation related to how the mathematical model was built. The three methods in this work were used due to its simplicity and accuracy. To develop this method only the first two moments are required, the mean values and the standard deviation.

3.1 First Order Reliability Method – F.O.R.M.

In this method, the estimates of the mean and the variance of the distribution function of g(X) are carried out using the mean vector and the covariance matrix associated to the random variables of the problem (Ferreira, 1997).

ISSN 2176-5480

Expanding g(X) in Taylor series around the average values of X, represented by $\hat{\boldsymbol{X}}$, and limiting the series to the linear terms, the first order approaches of the g(X) mean and variance will be defined by the Eqs. (16) and (17).

$$E[g(X)] = g(\hat{X}) = G(\hat{x}_1, \hat{x}_2, \hat{x}_3, \dots, \hat{x}_n) \quad (12)$$

$$Var[g(X)] = \sum_{i=1}^{n} \sum_{j=1}^{n} \left(\frac{\partial g(\hat{X})}{\partial x_i} \right) \cdot \left(\frac{\partial g(\hat{X})}{\partial x_j} \right) \cdot Cov[x_i, x_j] \quad (13)$$

If g(X) is represented by any probability distribution, the failure risk will be quantified by probability P(g(X) < E[g(X)]. However, assuming that such distribution is approximately normal with mean *E[g(X)]* and standard deviation $Var[g(X)]^{1/2}$, the failure risk will be assessed directly by the reduced normal distribution, that is, through the Eq. (14).

$$P_f = 1 - \Phi(\beta) \quad (14)$$

where β is a new risk failure measurement called reliability index, defined by Eq. (15).

$$\beta = \frac{E[g(X)]}{Var[g(x)]} \quad (15)$$

The FORM method is typically used due to simplicity of implementation. However, the methodology is not accurate to estimate the failure probability in limit state functions that has a nonlinear behavior or has some variables that are non-normal.

3.2 Second Order Reability Method – SORM

In SORM method, it is also estimated the mean and the variance of the distribution function of g(X) using the mean vector and the covariance matrix associated to the random variables of the problem. However, unlike the FORM method, the SORM method uses expansions in Taylor series around the average values of X, represented by $\hat{X}$, limiting the series to the second order terms (Ferreira, 1997). This approach improves the FORM result by including additional information about the curvature of the limit state function, LSF. For the fatigue problem studied, the covariance between the variables involved is null, and it is assumed that all variables involved are normally distributed. The second order approaches of the g(X) mean and variance for these conditions are defined by the Eq. (16) and (17).

$$E[g(X)] = g(\hat{X}) + \frac{1}{2} \cdot \sum_{i=1}^{n} \left(\left(\frac{\partial^2 g(\hat{X})}{\partial x_i^2} \right) \cdot Var[x_i] \right) \quad (16)$$

$$Var[g(X)] = \sum_{i=1}^{n} \left(\left(\frac{\partial g(\hat{X})}{\partial x_i} \right)^2 \cdot Var[x_i] + \frac{3}{4} \cdot \left(\frac{\partial^2 g(\hat{X})}{\partial x_i^2} \right)^2 \cdot [Var(x_i)]^2 \right) + \sum_{i \neq j} \left(\left(\left(\frac{\partial^2 g(\hat{X})}{\partial x_i \partial x_j} \right)^2 + \frac{1}{2} \cdot \frac{\partial^2 g(\hat{X})}{\partial x_i^2} \cdot \frac{\partial^2 g(\hat{X})}{\partial x_j^2} \right) \cdot Var(x_i) \cdot Var(x_j) \right) \quad (17)$$

Similarly to the FORM method, the relation between the failure probability, P_f, and the reliability index, β, is assessed according to Eq. (14).

3.3 Monte Carlo Method

The Monte Carlo technique is a reference method in reliability analysis. The methodology is a reference due to a high accuracy obtained for reliability. Basically, the Monte Carlo simulation is sampling processes that are used to estimate the unsatisfactory performance probability of a structure. The basic random variables in state limit equation are randomly generated (Press et al. 1992; Ayyub and McCuen 1997; Ayyub and Chao 1994) and used to estimate the fraction of cases that resulted in unsatisfactory performance. Assuming n_a to be the number of simulation cycles for which g(X) < 0 in a total N simulation cycles, then an estimate of the mean unsatisfactory performance probability can be expressed as

$$P(g < 0) = \frac{n_a}{N} \tag{18}$$

The estimated unsatisfactory performance probability, *P(g < 0)*, should approach the true value for the population when N approaches infinity. For that reason, the Monte Carlo technique has a high computational cost.

4. FATIGUE FAILURE MODELING

Considering a cyclic load history with non-null mean stresses, the fatigue failure condition is defined by Eq. (1) or Eq. (4). With base in those fatigue endurance criteria, the construction of a model of reliability estimate can be carried out as: considering a general loading condition to result in the pair (σ_m ,σ_a), defined as load point. Also considering that the load line that cross the load point will intercept the fatigue failure curve in the position (S_m, S_a), defined as strength point. Now, admitting that the distance between the loading point and the strength point can be used to express the safety condition regarding fatigue. Like this, when expressing the distances of the origin of the coordinate system to the load point and the strength point are defined, respectively, associated functions the demand, D, and the capacity, C, as illustrated in Fig. 2. In other words, the state limit function will be represented by the Eq. (19).

$$g(X) = \sqrt{{S_m}^2 + {S_a}^2} - \sqrt{{\sigma_m}^2 + {\sigma_a}^2} \tag{19}$$

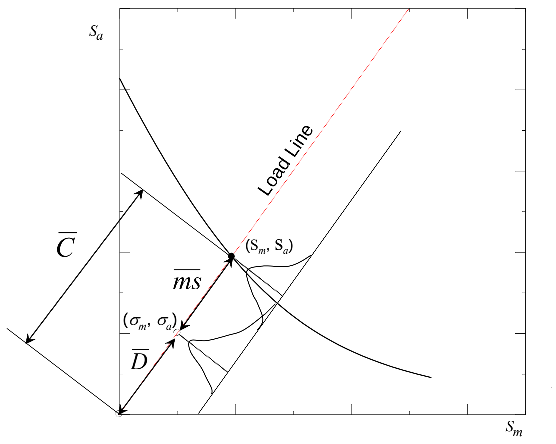

Figure 2 - Geometric characterization of capacity and demand

Considering the functional relation of the ordinate pairs (S_m, S_a) and (σ_m, σ_a) is expressed by Eq. (20), the Goodman, Gerber and Walker models, the components S_a and S_m will be written by Eq. (21) to (26):

$$S_a = \frac{\sigma_a}{\sigma_m} \cdot S_m \tag{20}$$

$$S_m|_{Goodman} = \frac{\sigma_m}{\frac{\sigma_a}{S_{ar}} + \frac{\sigma_m}{S_{ut}}} \tag{21}$$

$$S_a|_{Goodman} = \frac{\sigma_a}{\frac{\sigma_a}{S_{ar}} + \frac{\sigma_m}{S_{ut}}} \tag{22}$$

$$S_m|_{Gerber} = \frac{1}{2} \cdot \left[\sqrt{\left(\frac{\sigma_a \cdot {S_{ut}}^2}{\sigma_m \cdot S_{ar}}\right)^2 + 4 \cdot {S_{ut}}^2} - \frac{\sigma_a \cdot {S_{ut}}^2}{\sigma_m \cdot S_{ar}} \right] \tag{23}$$

$$S_a|_{Gerber} = \frac{\sigma_a}{2 \cdot \sigma_m} \cdot \left[\sqrt{\left(\frac{\sigma_a \cdot {S_{ut}}^2}{\sigma_m \cdot S_{ar}}\right)^2 + 4 \cdot {S_{ut}}^2} - \frac{\sigma_a \cdot {S_{ut}}^2}{\sigma_m \cdot S_{ar}} \right] \tag{24}$$

$$S_m|_{Walker} = S_{ar} \cdot \frac{\sigma_m}{\sigma_a} \cdot \left(\frac{\sigma_m}{\sigma_a} + 1\right)^{\gamma-1} \quad (25)$$

$$S_a|_{Walker} = S_{ar} \cdot \left(\frac{\sigma_m}{\sigma_a} + 1\right)^{\gamma-1} \quad (26)$$

In that work, in way to characterize the request function, it will be admitted that the shipment is described by the pairs of medium and alternate stress, respectively σ_m and σ_a, resultants of the stress history obtained by computational dynamic fluid and finite element method.

The gamma parameter, γ, from Eq. (25) and (26), and the endurance limits of the Eq.(21) to Eq.(26), S_{ar}, were calculated for this material by Silva (2009), and are exposed in the Tab. 1 and Tab. 2.

Table 1- Endurance limits for different loading ratio

R	A constant from a $S_{ar}=A.N^b$ regression of S-N curve. [MPa]		b exponent from a $S_a=A.N^b$ regression of S-N curve.		Endurance limit to 10^6 cycles [MPa]		Endurance limit to 2.10^6 cycles [MPa]	
	Mean	Standard deviation	Mean	Standard deviation	Mean	Standard deviation	Mean	Standard deviation
-1	1636.34	109.33	-0.1048	0.0055	384.60	26.51	357.35	26.76
- 2/3	1328.24	195.29	-0.0972	0.0117	346.87	19.29	324.28	20.40
- 1/3	1213.52	430.64	-0.1093	0.0272	267.89	23.91	248.34	26.01
0	1284.51	229.15	-0.1186	0.0147	249.57	28.11	229.87	28.80
1/3	563.79	91.3	-0.0785	0.0129	190.49	9.29	180.40	10.20
2/3	197.38	129.55	-0.0271	0.0497	135.66	16.63	133.14	19.05

Table 2 – Parameter gamma that characterize Walker's model

Parameter	Expected value	
	Mean	Standard deviation
γ	0.3658	0.004

The endurance limit was changed by a surface factor according Shigley (2005), whose characteristics statistics are presented in Tab.3.

Table 3 – Probabilistic characteristcs of operational parameter

Parameter	Mean	Coefficient of Variation (%)	Probability Distribution
K_a	$4.45 \cdot S_{ut}^{-0,265}$	5.8	Lognormal

5. TRANSIENT ANALYSIS BY THE FINITE ELEMENT METHOD

The static load distribution on the Kaplan turbine blade of the hydroelectric plant of Coaracy Nunes, hydro generator 3, was obtained by a numerical simulation CFX software (Soares et al, 2005), and the Tab. 4 present the data obtained from the Manual Voith-Hydro-UHE Coaracy Nunes, 1998.

The simulation was performed by LEA, Laboratório de Energia e Ambiente, UnB, in the commercial software CFX 5.5.1. The simulation is based on the finite volume method, with a hexahedra elements mesh generated in the ICEM CFD 4.2.2 (Moura, 2003). The pressure field on the blade obtained with this methodology can be seen in Fig. 3.

ISSN 2176-5480

Table 4 – Hydro generator's work condition studied.

Working Condition		Turbine's characteristics	
Nominal Power [MW]	29.5	Stator height [m]	2.78
Nominal height [m]	21.9	Distributor height [m]	1.703
Nominal outflow [m^3/s]	143	Blade's inclination angle	13°
		Distributor's opening angle	67.5°

The finite element mesh of 9649 elements and 2904 nodes, Fig. 4, was used in the finite element analysis with the ANSYS 5.4 software. The Solid 72 element was used. It's a four-node isoparametric tetrahedral element which has 6 degrees of freedom per node.

For the transient analysis, the static load was modified in the surfaces showed in Fig. 4, adding to the nominal pressure loading blocks in that the pressure amplitudes vary of plus and minus 10 or 20% in relation to the medium pressure, generating the typical pressure history showed in Fig. 5. The dominant frequency of the load is 1.25 Hz. From time t = 0 to t = 1 integration step is of 0.05 s, and a total of 20 iterations. For time t = 1 s to t = 16 s, an integration step is of 0.02 s and a total of 800 iterations were calculated. A damping $\xi = 0.06$ was considered in the transient analysis.

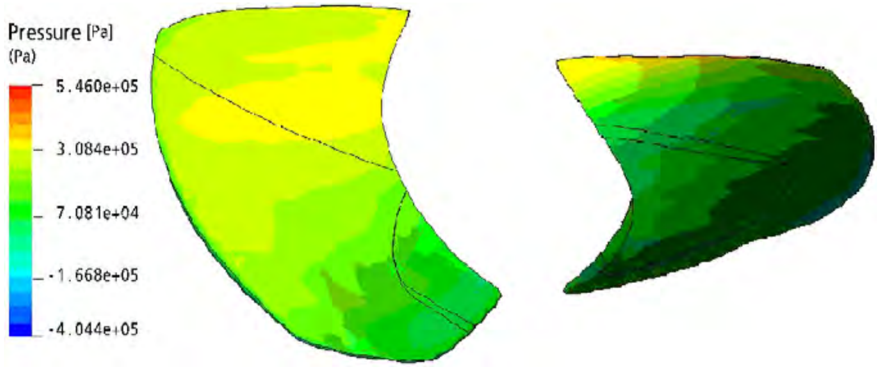

Figure 3 - Pressure field obtained by the CFD simulation (Soares et al, 2005).

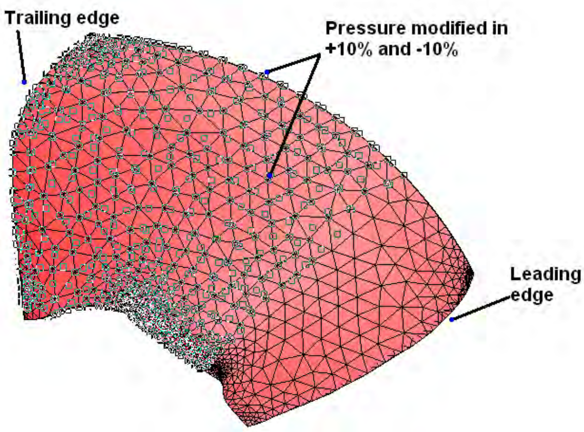

Figure 4 - Finite element mesh and region of the blade where the static load was modified (Soares et al, 2005).

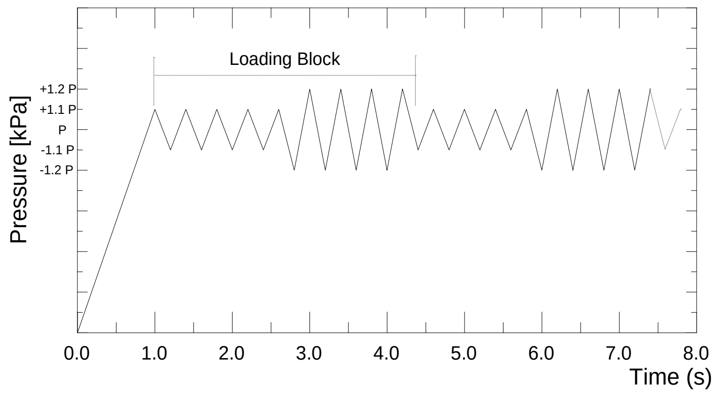

Figure 5 - Pressure history applied on the blade for the transient analysis (Soares et al, 2005).

5.1 5.1 Transient analysis results

Figure 6 shows the stress field on the blade in time t=3.02 *s*.

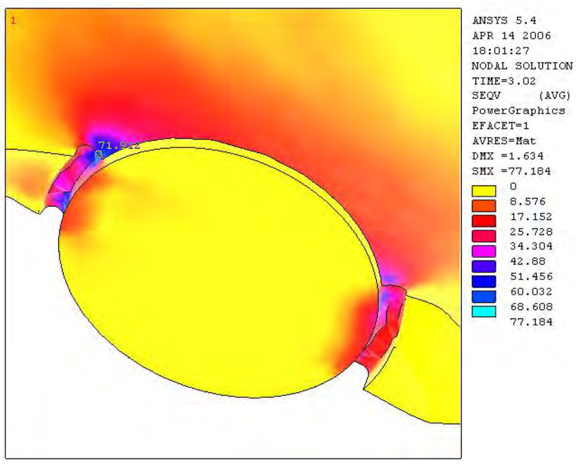

Figure 6 - Von Mises stress field over the blade in time t=3.02 s

After rain-flow counting of the stress history applied on hot point, showed in Fig. 7.a, it was possible to build a data base with approximately 50 load point, showed Fig. 7.b. Based on those points it was possible to identify the statistical characteristics of the mean and alternate stresses present in the loading, whose results are presented in Tab. 5.

Table 5 - Statistical behavior of Stress Components

Stress Component	Central Tendency		C.V. [%]	Probability Distribution
	Mean [MPa]	Median [MPa]		
σ_m	133.6	134.0	16.1	Normal
σ_a	45,9	46,1	36	Normal

ISSN 2176-5480

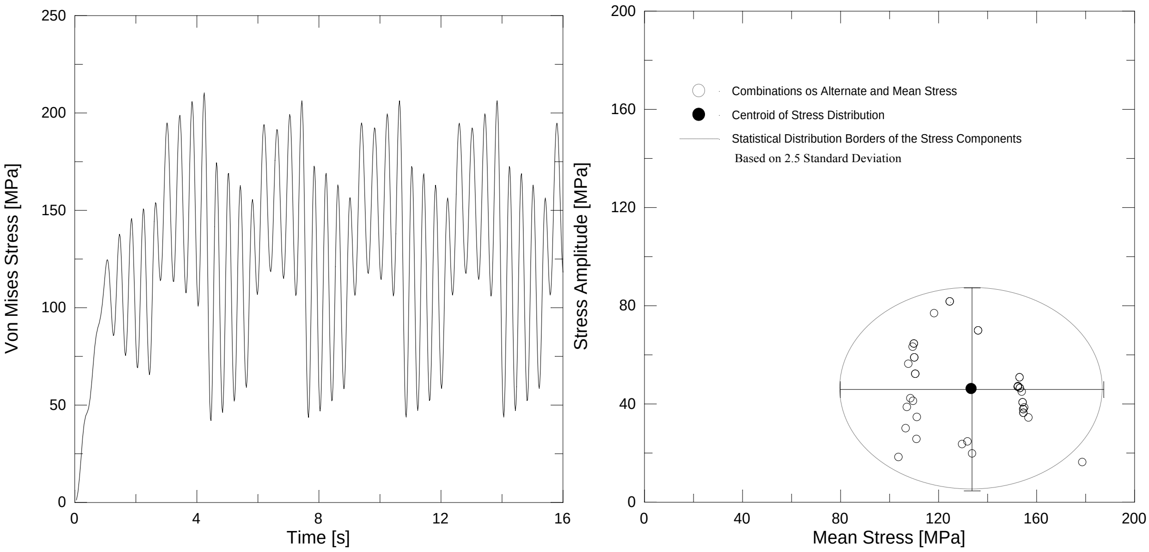

(a) (b)

Figure 7 - Stress History and the Mean and Alternate Stress Dispersion Diagram Based on Rainflow Counting Technical Applied on Hot Spot.

6. DETERMINATION OF THE BLADE'S MATERIAL PROPERTIES

The material used in the development of this research was the ASTM A743 CA6NM steel alloy, kindly supplied by a turbine specialist industry. This type of steel is used in the manufacturing of structural components that request a high mechanical and corrosion resistance, being used in hydraulic turbine blades and other components. The mechanical and chemical properties of the used material, given by the manufacturer, are presented in Tab. 6 and 7. Simple tension tests were used to validate the former estimates of the material yield strength and ultimate strength. The tests were performed with two millimeters per minute, with displacement control, in a MTS 810 universal testing machine.

Table 6 - Chemical Composition (%)

Element	C	Mn	Si	Cr	Ni	Mo	P	S	Cu	V
Mass (%)	0.016	0.7	0.43	12.5	3.7	0.45	0.03	0.016	0.15	0.03
Tolerance	±0.002	±0.01	±0.02	±0.02	±0.01	±0.01	±0.01	±0.001	±0.01	±0.01

Table 7 - Mechanical properties

S_{ut} (MPa)	S_y (MPa)	R.A. (%)	Elongation(%)
942	575	15	35

7. RESULTS

The results obtained for the transient analysis were used to characterize the demand function. The capacity demand is determined by the blade's material properties and by the mean and alternate stresses acting on it. All parameter were considered random variables with normal or lognormal distributions. The blade's reliability was calculated through the Goodman, Gerber's and Walker models for the fatigue failure mode by the FORM, SORM, and Monte Carlo technique. Tab. 8 shows the reliability for each fatigue model used.

ISSN 2176-5480

Table 8 - Reliability for each fatigue model and reliability method

Fatigue Model	Reliability (%)		
	Monte Carlo	FORM	SORM
Goodman	100	99.925589	99.969541
Gerber	100	99.988032	99.996173
Walker	99.999570	98.230000	99.440000

By the reliability results, it is possible to see that Monte Carlo prediction is always near from FORM and SORM methods. This difference, however small, is due to the fact that the distributions, constructed using the mean and variance estimated by FORM and SORM methods, are not compatibles with the distribution of the limit state function. The Figure 8 demonstrates that difference using Walker's model for each reliability method used.

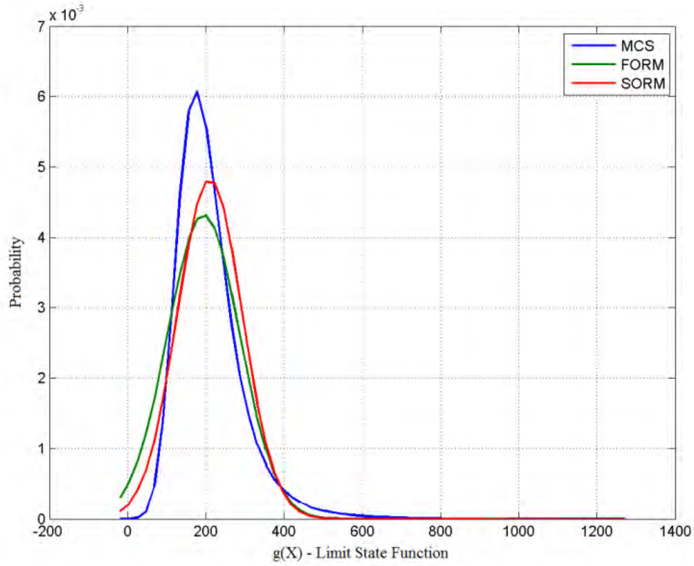

Figure 8 - Distribution of g(X) according to reliability methods.

For the evaluation of the reliability through the technique of simulation of Monte Carlo it was used 10^8 simulations cycles. To evaluate the influence of the number of draw in Monte Carlo reliability, it was plotted the evolution of failure probability for the Walker's model.

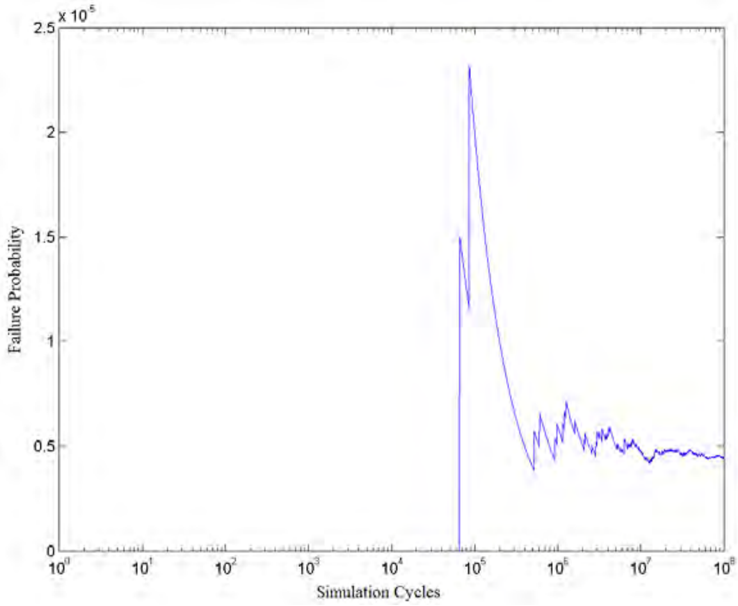

Figure 9 - Failure probability by Monte Carlo simulation - Walker

ISSN 2176-5480

8. CONCLUSIONS

A complete methodology to determine the structural reliability of a Kaplan hydro turbine blade was presented in this paper from the load definition to the modeling of the failure criteria by probabilistic techniques and the characterization of the demand and capacity parameters. The cyclic load model is hypothetical and the structure is not likely to fail according to the presented results.

The limit state function showed nonlinear behavior. Aware that the FORM and SORM methods depart from the principle that the limit state function is linear and its associated variables are Gaussian, it is understandable that distributions proposed by those methods are not in accordance with the distribution from Monte Carlo, as presented in Fig.(8). As the figure revels, only a small piece of the tail's distribution is smaller than zero, and corresponds to the failure condition. In this case, even if the values of the estimated reliabilities are close, it is indicate the use of the Monte Carlo method due to higher accuracy.

Based in the Fig.(9) analysis, it is verified that, for the conditions used in that work, the reliability estimate will only be considered secure when the number of trials goes superior to 10^7.

9. ACKNOWLEDGEMENTS

The authors acknowledge Centrais Elétricas do Norte do Brasil S.A – Eletronorte and Voith Siemens of Brazil for supporting the project and technical data.

10. REFERENCES

Harr, M.E., 1987, “Reliability-Based Design in Civil Engineering”, Dover Publications, Inc., New York, Chapters 3 and 4.

Mamiya E. N. and Souza C., 2004, “Relatório Parcial do Projeto UnB/Eletronorte Fadiga de Máquinas Rotativas, Incorporação dos Modelos de Fadiga Multiaxial ao Programa de Elementos Finitos”, Grupo de Mecânica dos Materiais, Dep. de Engenharia Mecânica, Universidade de Brasília.

Manual Voith-Hydro-UHE Coaracy Nunes, 1998. Máquina 3 .

Marin, Joseph, 1962, “Mechanical Behavior of Engineering Materials”, Prentice-Hall, Englewood Cliffs, N.J., p. 224.

Moura, M. D., 2003, “Assessment of Turbulence Modeling for CFD Simulation in Hydroturbines: Draft Tube”, Proceedings of the 17thCOBEM

Shen, W. and Soboyejo, W. O., 2001, “Probabilistic Modeling of Fatigue Crack Growth in T1 – 6 Al – 4V”, International Journal of Fatigue, vol 23, Issue 10, November, pp 917-925.

Soares, A. A. B. et al, 2005, “Methodologies for Load Distribution on a Kaplan Hydro Turbine Blade”, 2481, Proceedings of the 18th COBEM.

Ferreira, J. L. A., Souza, A. B. , Leite, D. A , Oliveira, A. B., Carloni, V., 2005. Structural integrity analysis of the main bearing cap screws of the turbo-diesel engine crank shaft. Engineering Failure Analysis, v. 12, n. 2, p. 273-286..

Ayyub, B. M., and Chao, R.-J. ,1994. “Probability distributions for reliability based design of naval vessels,” CARDEROCKDIV-U-SSM-65-94/12, Naval Surface Warfare Center, U.S. Navy, Carderock Division, Bethesda, MD.

Ayyub, B. M., and McCuen, R. H. ,1996. Numerical methods for engineers. Prentice Hall, Upper Saddle River, NJ.

Press, W. H., Teukolsky, S. A., Vetterling, W. T., and Flannery, B. P. (1992). Numerical recipe in FORTRAN: The art of scientific computing. 2nd ed., Cambridge University Press, New York.

Shigley, J. E.,2005. “Projeto de Engenharia Mecânica”, Bookman, Michigan – USA

Ferreira, J. L. A., 1997. “Um modelo para previsão da incerteza do dano por fadiga”. Ph.D. thesis, Pontifícia Universidade Católica do Rio de Janeiro, Rio de Janeiro Brasil.

Silva, B. L., Ferreira, J. L. A., Oliveira, F., Araújo, J. A., 2009. "The effect of mean stress on the fatigue behabior of ASTM A743 CA6NM alloy steel".